

BIO-INSPIRED CERAMIC/CARBON COMPOSITES

**Prof. Nicole Grobert
Prof. Richard Todd**

**Department of Materials
University of Oxford**

Approved for Public Release, Distribution Unlimited

Report: May 2013

Report Documentation Page			<i>Form Approved OMB No. 0704-0188</i>	
<p>Public reporting burden for the collection of information is estimated to average 1 hour per response, including the time for reviewing instructions, searching existing data sources, gathering and maintaining the data needed, and completing and reviewing the collection of information. Send comments regarding this burden estimate or any other aspect of this collection of information, including suggestions for reducing this burden, to Washington Headquarters Services, Directorate for Information Operations and Reports, 1215 Jefferson Davis Highway, Suite 1204, Arlington VA 22202-4302. Respondents should be aware that notwithstanding any other provision of law, no person shall be subject to a penalty for failing to comply with a collection of information if it does not display a currently valid OMB control number.</p>				
1. REPORT DATE MAY 2013	2. REPORT TYPE	3. DATES COVERED 00-00-2013 to 00-00-2013		
4. TITLE AND SUBTITLE Bio-Inspired Ceramic/Carbon Composites		5a. CONTRACT NUMBER W911NF-12-1-0616		
		5b. GRANT NUMBER		
		5c. PROGRAM ELEMENT NUMBER		
6. AUTHOR(S)		5d. PROJECT NUMBER		
		5e. TASK NUMBER		
		5f. WORK UNIT NUMBER		
7. PERFORMING ORGANIZATION NAME(S) AND ADDRESS(ES) University of Oxford, Department of Materials & Corpus Christi College, Oxford OX1 3PH, UK,		8. PERFORMING ORGANIZATION REPORT NUMBER ; 1580-EN-01		
9. SPONSORING/MONITORING AGENCY NAME(S) AND ADDRESS(ES) Army Engineer Research & Development Center - International Research Office, ERDC-IRO, ATT: RICHMOND, Unit 4507, APO, AE, 09421		10. SPONSOR/MONITOR'S ACRONYM(S)		
		11. SPONSOR/MONITOR'S REPORT NUMBER(S) 1580-EN-01		
12. DISTRIBUTION/AVAILABILITY STATEMENT Approved for public release; distribution unlimited				
13. SUPPLEMENTARY NOTES				
14. ABSTRACT				
15. SUBJECT TERMS				
16. SECURITY CLASSIFICATION OF:			17. LIMITATION OF ABSTRACT Same as Report (SAR)	18. NUMBER OF PAGES 10
a. REPORT unclassified	b. ABSTRACT unclassified	c. THIS PAGE unclassified	19a. NAME OF RESPONSIBLE PERSON	

Chemical vapour deposition growth of multi-walled carbon nanotubes in freeze casted alumina scaffolds

The influence of different parameters including catalyst concentration, infiltration time, and carbon sources on the quality and homogeneity of the *in situ* grown carbon nanotubes (CNTs) was evaluated.

The synthesis approach we used was based on *in situ* aerosol assisted chemical vapour deposition using alumina scaffolds (supplied by Imperial) as substrate materials. Fe_2O_3 nanoparticles with sizes between 5-7nm were freshly prepared, dispersed in cyclohexane and, used as metal catalysts. The infiltration of the scaffolds with catalyst particles was conducted for different times and concentrations. The as-infiltrated scaffold placed in a quartz tube inside a furnace and heated to 800°C at a rate of 10°C/min in an Ar flow of 1000 sccm. Once the furnace reached 800°C and the temperature was stable the substrate was kept for a further 10-15 min, then the gases were switched to Ar 200 sccm, H_2 150 sccm, and 50 sccm acetylene (C_2H_2) which was used as carbon source. Following the synthesis, the sample was cooled down at a rate of *ca.* 2.5°C/min under Ar (1000 sccm, more details about the infiltration process and the synthesis are in the previous report).

Fe_2O_3 nanoparticles with concentrations ranging from 0.2 to 0.02 M were used. As a first approach, the infiltration time was 7 days for all the samples. For 0.2, 0.1 and 0.06M concentrations the results were very similar. The outside of the scaffold (directly in contact with the catalyst solution) appeared completely covered with CNTs while the inside walls showed less CNT coverage with a high trend to agglomerate at the grain boundaries. Figure 1 shows the scanning electron micrograph (SEM) images of the as-synthesized hybrid scaffold/CNTs for 0.1M Fe_2O_3 nanoparticles concentration.

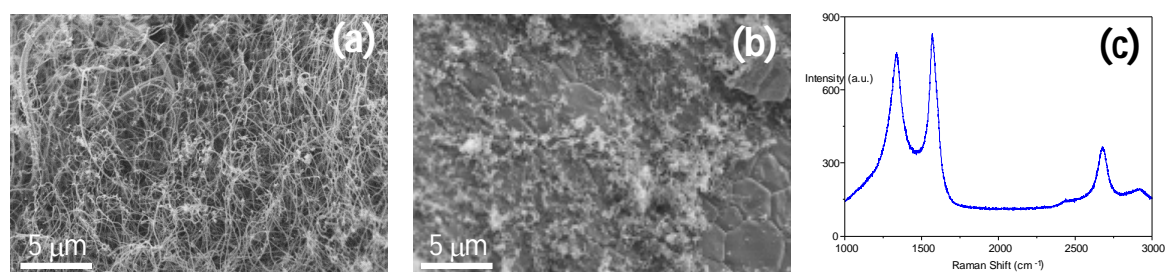


Figure 1. (a) SEM micrograph of the outside walls of the scaffold, (b) SEM micrograph of the inner walls and (c) corresponds to the Raman Spectra of the synthesized CNTs.

The quality of CNTs was evaluated by Raman Spectroscopy, in all the prepared samples the ratio D/G ~ 1, indicating a high concentration of defects independently of the concentration of the catalyst. Figure 1c shows the Raman spectra of the CNTs synthesized from a 0.1M concentration of catalyst.

When lower concentrations of Fe_2O_3 nanoparticles were used, *e.g.* 0.04 and 0.02M, under the same growth conditions, a graphite layer covering all the surface of the scaffold was observed but there was no evidence of CNTs.

The observed gradient in the quantity of the CNTs that formed on the outside and those that grew on the inside of the scaffold could be due to inefficient infiltration or an insufficient infiltration time. Therefore, the same synthesis process was performed in one scaffold after two months and a half (83 days) soaking in a 0.2M catalyst solution.

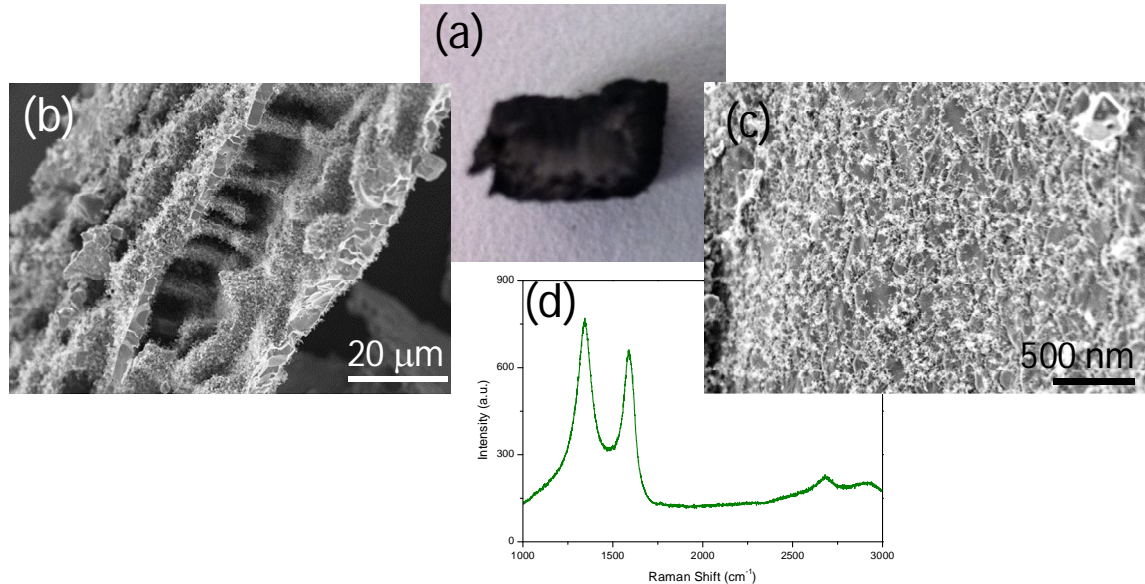


Figure 2. (a) Optical image of the hybrid Al_2O_3 scaffold/CNTs synthesized from a 0.1M Fe_2O_3 catalyst solution after 83 days of infiltration. Micrographs b and c show the outside and inner walls of the scaffold after the synthesis, respectively. (d) Raman spectrum of the as-synthesized CNTs.

Figure 2a shows a picture of the hybrid scaffold/CNTs synthesized after 83 days of catalyst infiltration process cut in half, the change in concentration can be observed with the naked eye. SEM studies of the sample confirm these findings - while the outside walls (Fig. 2b) are fully covered with CNTs while the inner walls (Fig. 2c) exhibit much fewer.

Raman spectroscopy (Fig. 2d) revealed a D/G ration of > 1 on average for all spectra, highlighting the high defect concentration in the CNTs synthesized by this method.

Based on the findings two limitations were identified for *in situ* growth of CNTs to form the hybrid materials, the first one is the quality of the CNTs and the second the gradient in concentration found along the scaffold, independent of the catalyst concentration or the infiltration time. In order to overcome the first one a different precursor was used. The approach we used was also based on *in situ* aerosol CVD synthesis but in this case the scaffold was infiltrated simultaneously with the catalyst and carbon source (solution of 3 wt% ferrocene ($\text{Fe} [\text{C}_5\text{H}_5]_2$) in toluene ($[\text{C}_6\text{H}_5\text{CH}_3]$)). The CVD experimental set-up consisted of a piezoelectric driven aerosol generator, a quartz tube (2.2 cm inner diameter), an 80 cm long horizontal tube furnace, gas flow controllers, and an acetone gas trap. The alumina scaffold was placed into the quartz tube outside of the furnace; the furnace was then pre-heated to 800°C under Ar flux of 4000 sccm, once the temperature was stable the flux was changed to 200 sccm of acetylene (to avoid the oxidation/sublimation of ferrocene) and Ar (2000 sccm) of, after this, the quartz tube was shift inside the furnace for 10 min. Finally the system was cooled down at 2.5 °C/min keeping the same Ar flow rate.

Scanning electron microscopy studies of these samples are shown in figure 3: micrographs a and b show different areas of the outside walls of the scaffold; in some areas there is a high density of CNTs while in others (b) the density is much lower, however nucleation points appear all along the surface indicating a possible lack of time for the CNT formation inside the scaffold. On the other hand, the inside walls of the scaffold appear graphitized (Fig. 3c) and only in specific areas small CNTs can be observed (Fig. 3d). Raman study to evaluate the quality of the as-synthesized CNTs is in progress.

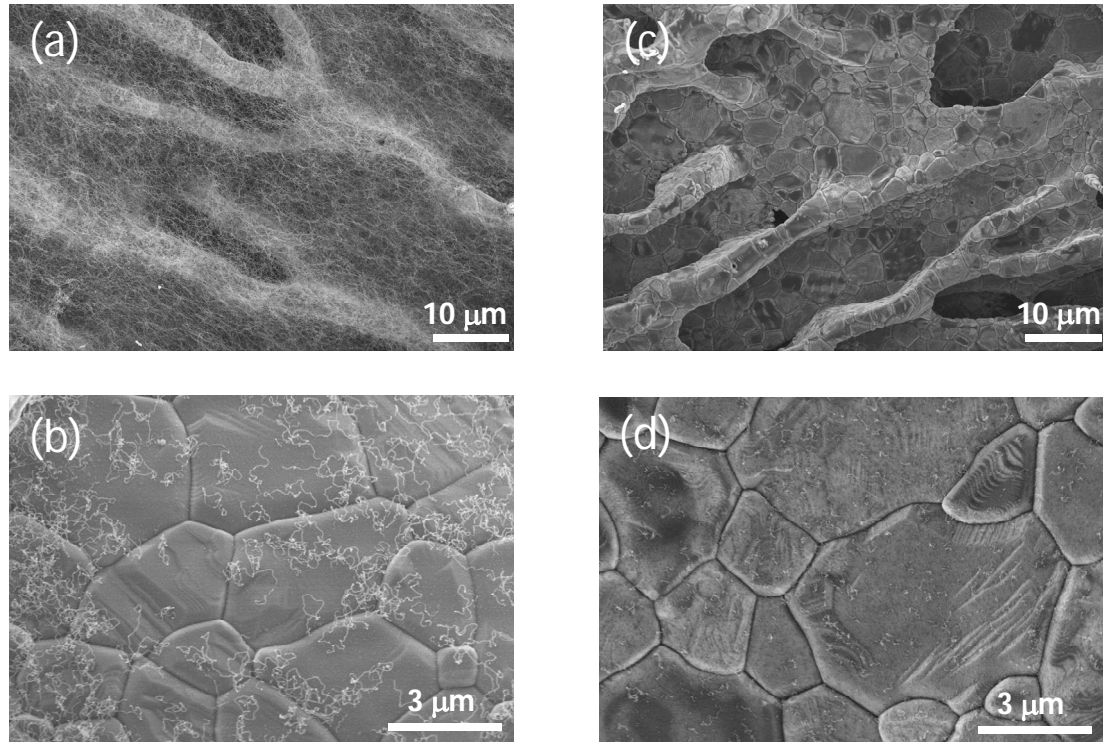


Figure 3. SEM micrographs of the hybrid CNT/Al₂O₃ scaffold using the solution ferrocene/toluene as catalyst/carbon source, a and b shows images corresponding to the outer walls while c and d corresponds to the inner walls of the scaffold.

Study by High-Resolution Microscopy (HRTEM) of the CNTs/Al₂O₃ interface

In order to gain a better understanding of the CNTs/Al₂O₃ interface structural studies by high-resolution electron microscopy (Jeol 3000F) were performed on the hybrid material synthesized using 0.2M Fe₂O₃ nanoparticles in conjunction with acetylene at 800°C for 10 min.

CNTs with different diameters could be observed; in general they are surrounding Al₂O₃ grains as can be seen in figure 4(A). The darkest contrast corresponds to the metal catalyst nanoparticles located at the tip, curvature or base of the CNTs. Therefore, it is likely that growth scenarios following different mechanisms are taking place. Almost all of the studied CNTs exhibit compartments (Fig. 4B), e.g. the inner channel is separated in different parts by graphitic layers. A more detailed study is necessary to confirm these observations.

It is important to note that the presence of a graphitic layer surrounded the Al₂O₃ grain. This layer can clearly be observed on image 4D and in greater detail in 4E where the graphitic layers can be distinguished. This layer has been observed in other grains and it is probable

that plays an important role in the growth of CNTs in the alumina scaffold, although all of this must be considered carefully in further studies with different samples.

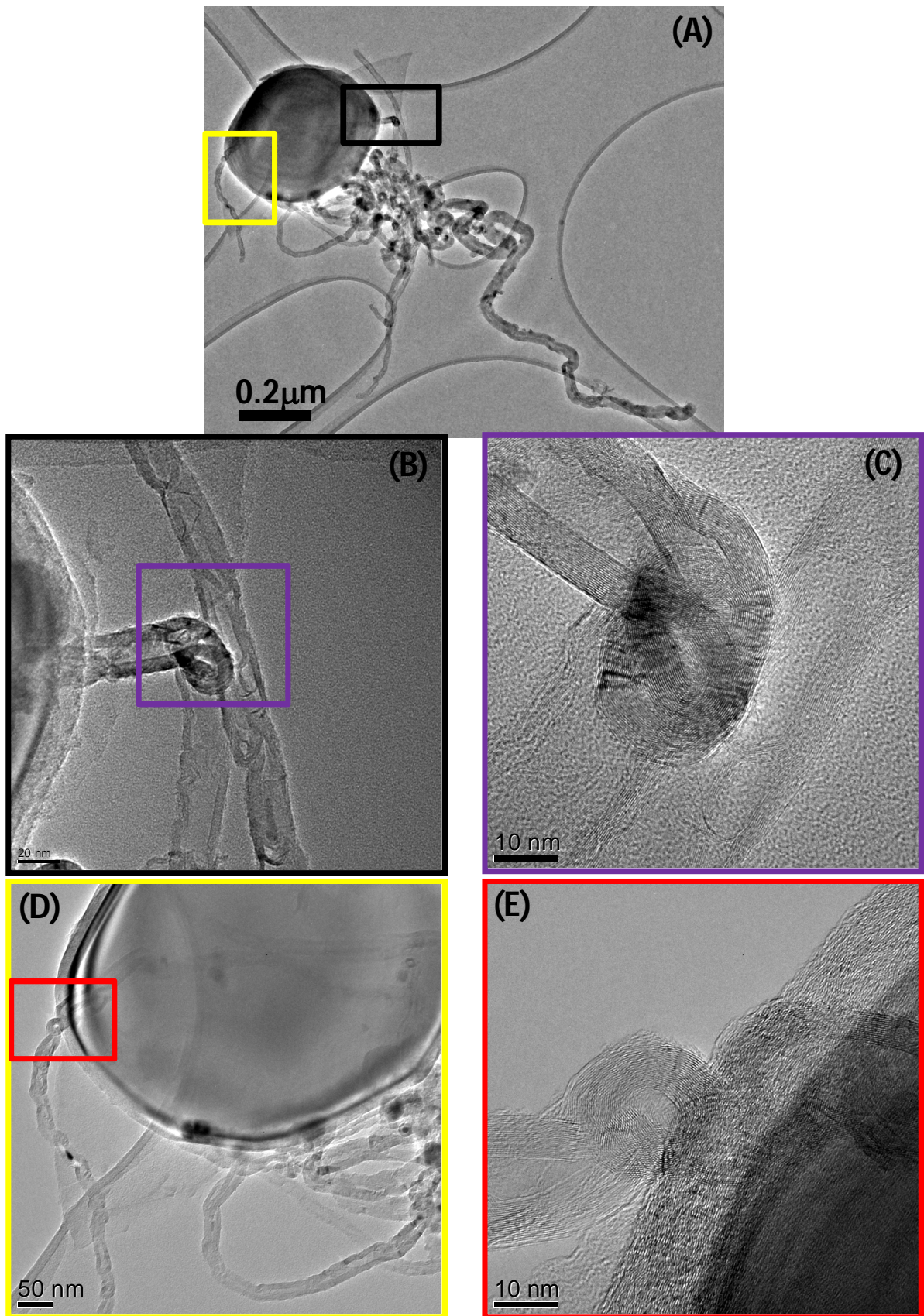


Figure 4. HRTEM images of the CNTs (B and C) and the interface CNTs/ Al_2O_3 (D and E).

Conclusions and future work

Two different types of catalyst/carbon sources were studied and further work needs to be performed regarding to the infiltration method in order to overcome the gradient issue. Since we were able to show that the infiltration did not improve the overall homogeneity between the outer and inner walls, a vacuum infiltration system is being designed already in order to improve these results. Past experiments showed that when ferrocene/toluene as catalyst/carbon sources is employed the quality of the CNTs improves. Nevertheless adjustment of the synthesis conditions is needed.

Interfaces CNT/Al₂O₃ particles must be studied in greater detail in order to understand the growth mechanism of the CNTs under these conditions and in order to optimize the synthesis of the bio-inspired hybrid materials.

Infiltration of CNTs carpets with Al₂O₃ by sol-gel will be also performed in order to better understand the links between CNTs and the ceramic when the CNT is previously synthesized.

Spark Plasma Sintering of SiC/CNTs composites

Composites containing 5% of CVD MWCNTs and 95% of SiC nanoparticles (size ~ 100nm) were prepared by Spark Plasma Sintering under different conditions. Table I shows the conditions of the prepared samples.

Table I. SiC/CNTs composites compositions and SPS conditions

SAMPLE	SAMPLE COMPOSITION			T (°C)	T (min)	P (MPa)
	CNTs (%)	SiC (%)	Additives (%)			
1	-	100	-	1900	15	70
2	5	95	-	1900	15	70
3	5	95	-	2100	15	70
4	5	95	4% Y ₂ O ₃ 6% Al ₂ O ₃	1900	15	70
5	-	100	4% Y ₂ O ₃ 6% Al ₂ O ₃	1900	15	70

CNTs were dispersed in isopropanol; the suspension was sonicated for 2 min using an ultrasound probe followed by sonication in an ultrasound bath at room temperature for 2 hours. The corresponding amount of SiC was then added to the suspension, as well as the additives when necessary (additives were added to help to improve the sintering increasing the density values), and the mixture continuously stirred until the solvent was completely evaporated. Finally, the slurries were dried in an oven at 60°C for 48 hours. The obtained powders were sintered by SPS with the conditions detailed in table I.

Density of the samples was measured by the Archimedes' method. The relative density was calculated using the theoretical density of each composition, Young's modulus was determined by the Impulse Excitation Technique (IET) and fracture strength by four point bending tests. Table II shows the obtained values.

Table II. Density, relative density, Young's modulus and fracture strength values of the composites sintered by SPS. The error corresponds to the standard deviation.

Composite	Density (g/cm ³)	Relative density (%)	Young's modulus (GPa)	Fracture strength (MPa)
1	2.84 ± 0.08	88 ± 2	273 ± 9	342 ± 22
2	2.76 ± 0.02	92 ± 1	242 ± 3	248 ± 53
3	3.10 ± 0.02	103 ± 1 *	412 ± 12*	381 ± 34
4	3.05 ± 0.02	99 ± 1	297 ± 6	461 ± 26

Sample 5 is still under investigation.

The presence of CNTs increases significantly the density of the composite from 88 to 92% and an increase on the sintering temperature gives rise to a density higher than 100% (discussed below). On the other hand, the presence of additives keeping the temperature at 1900°C leads to a composite with 99%.

SiC Young's modulus is 420 GPa and its fracture strength 400-500 MPa, these values are similar to those obtained for the sample 3 (SiC/CNTs5%- 2100°C/70Mpa/15min), this fact join to the high density (over a 100%) might be due to the total or partially decomposition of the CNTs during the sintering process in such a way that the final amount of CNTs is lower than a 5% leading to erroneous data.

The comparison between the different values indicate that the presence of CNTs helps the sintering process and decreases the Young's modulus, keeping similar fracture strength values of dense SiC materials.

The microstructure of the composites is being studied; figure 5 shows the fracture surface of the samples 1, 2 and 3. The composite formed by SiC nanoparticles sintered at 1900°C (at Imperial) show a porous microstructure (fig. 5 a and b) as was expected from the obtained density value, the addition of 5% of CNTs with the same sintering conditions (fig. 5 c and d) leads to an evident grain growth; however a high degree of porosity still remains in the composite. An homogeneous distribution of CNTs is observed along the surface but the decrease in the fracture surface strength between these two materials can be explained by the presence of the CNTs in the porous areas and not between the sintering grains, at this stage the CNTs do not seem to have any or have a negative effect on the resistance of the material. When the sintering temperature is increased from 1900 to 2100°C fewer CNTs are present (fig. 5 e and f) confirming the partial decomposition of CNTs during the process; however the composite appear to be fully dense with the CNTs pulling out the fracture surface. The holes can be observed in this surface correspond to CNTs that have been completely pulled out and must be adhered to the other side of the surface. There is no evidence of CNTs parallel to the fracture surface.

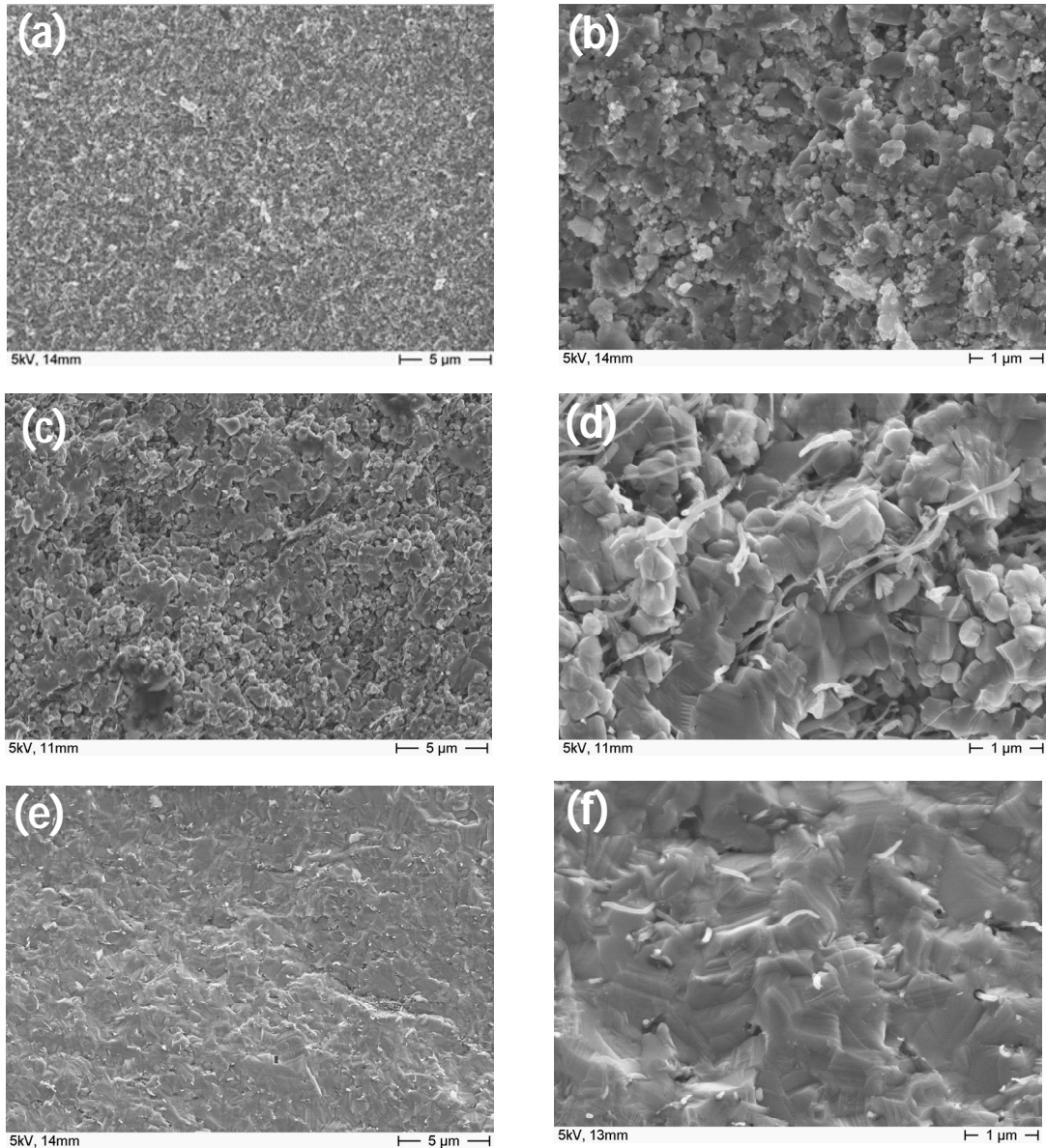


Figure 5. SEM micrographs of different composites sintered by SPS at 70 MPa for 15 min, the temperature changes depending on the material. (a) and (b) correspond to the SiC composite sintered at 1900°C, (c) and (d) SiC/CNT 5% sintered at 1900°C and (e) and (f) to the same composition sintered at 2100°C.

Conclusions and future work

The effect of the addition of CNTs in the synthesis of SiC composites has been evaluated leading to promising results regarding to the homogeneity of the nanotubes along the material. Raman spectroscopy needs to be performed in all the samples to establish the possible damage, if any, made to the CNTs. Moreover, a more detailed microscopy study is needed to understand the interfaces between the matrix and the nanotubes to determine the role they may have during the sintering process and the obtained mechanical response.

On the other hand, *in situ* CNTs growth on the SiC scaffolds synthesized by Eduardo Saiz's group will be done based on the previous results obtained with the Al₂O₃ regarding to the

infiltration process and with the growing on SiC nanoparticles (previous report), regarding to the synthesis conditions.

Infiltration of CNTs carpets with a polymer precursor of SiC is also one of the goals of this part of the project.